Tunable mechanical behavior of synthetic organogels as biofidelic tissue simulants

Z. Ilke Kalcioglu[1,+], Randy A. Mrozek[2,+], Roza Mahmoodian[1], Mark R.VanLandingham[2], Joseph L. Lenhart[2,]*, and Krystyn J. Van Vliet[1,]*

[1]*Department of Materials Science and Engineering, Massachusetts Institute of Technology, Cambridge, MA 02139 USA*
[2]*U.S. Army Research Laboratory, 4600 Deer Creek Loop, Aberdeen Proving Ground, MD 21005 USA*

+These authors contributed equally to the research.
*Corresponding author:

Krystyn J. Van Vliet: krystyn@mit.edu;
Address: 77 Massachusetts Avenue 8-237, Cambridge MA 02139 USA,
Phone: 617- 253-3315,
Fax: 617-253-8745

Joseph L. Lenhart: joseph.l.lenhart.civ@mail.mil;
Address: U.S. Army Research Laboratory, 4600 Deer Creek Loop, Aberdeen Proving Ground, MD 21005 USA
Phone: 410-306-1940
Fax: 410-306-0676

Keywords: tissue simulants, rheology, impact indentation, PDMS, soft tissues, energy dissipation

This manuscipt is submitted to be considered as an original article.

Word Count (Introduction through Discussion): 3980

Tunable mechanical behavior of synthetic organogels as tissue simulants compared to biological tissues

Z. Ilke Kalcioglu[1,+], Randy A. Mrozek[2,+], Roza Mahmoodian[1], Mark R.VanLandingham[2], Joseph L. Lenhart[2,]*, and Krystyn J. Van Vliet[1,]*

[1]*Department of Materials Science and Engineering, Massachusetts Institute of Technology, Cambridge, MA 02139 USA*
[2]*U.S. Army Research Laboratory, 4600 Deer Creek Loop, Aberdeen Proving Ground, MD 21005 USA*

+These authors contributed equally to the research.
*Corresponding authors e-mail: krystyn@mit.edu; joseph.l.lenhart.civ@mail.mil

ABSTRACT

Solvent-swollen polymer gels can be utilized as mechanical simulants of biological tissues to evaluate protective systems and assess injury mechanisms. However, a key challenge in this application of synthetic materials is mimicking the rate dependent mechanical response of complex biological tissues. Here, we characterize the mechanical behavior of tissue simulant gel candidates comprising a chemically crosslinked polydimethylsiloxane (PDMS) network loaded with a non-reactive PDMS solvent, and compare this response with that of tissue from murine heart and liver under comparable loading conditions. We first survey the rheological properties of a library of tissue simulant candidates to investigate the effects of solvent loading percentage, reactive functional group stoichiometry, and solvent molecular weight. We then quantify the impact resistance, energy dissipation capacities, and energy dissipation rates via impact indentation for the tissue simulant candidates, as well as for the murine heart and liver. We demonstrate that by tuning these variables the silicone gels can be engineered to match the impact response of biological tissues. These experiments inform the design principles required for synthetic polymer gels that are optimized to predict the response of specific biological tissues to impact loading, providing insight for further tuning of this gel system to match the impact response of other "soft tissues."

1. Introduction

The defense, law enforcement, automobile, and contact sports industries have identified a growing need for head and torso forms, and general testing media, that accurately mimic the rate-dependent mechanical response of the human body for assessment of new protective equipment and for understanding injury mechanisms in response to a broad range of impact, blunt trauma, and penetrating threats (Bertrand et al., 2008; Bresson and Frank, 2010; Roberts et al., 2007; Thali et al., 2002). Common simulants exploited in these forms for compliant tissues comprising skin, brain, muscle, and internal organs include ballistic gelatin, various rubbers, leather, silicone elastomers, soap, lard, and clay (Appleby-Thomas et al., 2011; Jussila et al., 2005; Merkle et al., 2008). In most cases, the tissue simulants are a crude representation of the biological tissue response; however, detailed assessment of protective equipment and injury mechanisms requires more accurate simulants that quantitatively mimic complex rate-dependent behavior of biological tissues. Therefore, a critical challenge for these applications is to develop environmentally stable, easily processable, and cost effective synthetic materials that recapitulate the mechanical response of biological tissues (Juliano et al., 2006; Moy et al., 2006) that are mechanically compliant and exhibit complex nonlinear, time-dependent deformation behavior (Bisplinghoff et al., 2009; Nicolle et al., 2010; Oliver et al., 2010; Saraf et al., 2007; Song et al., 2007; Storm et al., 2005; Weiss et al., 2002).

Many different gel chemistries offer novel methods to tune gel properties and better mimic the mechanical response of biological tissues. Examples include polybutadiene (Lenhart and Cole, 2006), epoxy (Mrozek et al., 2012), polyvinyl-alcohol (Stammen et al., 2001), physically associating gels (Seitz et al., 2009), and various hydrogels (Gong, 2010). Block copolymer-based gels containing a mid-block selective solvent have been explored explicitly for use as tissue simulants in head and torso forms (Juliano et al., 2006; Kalcioglu et al., 2011; Moy et al., 2006). The mechanical response of these materials can be tailored through solvent loading, the incorporation of diblock polymer, the ratio of the constituent blocks, and the manipulation of the block copolymer chemistry. However, those gels synthesized to date have not accurately mimicked the response of soft tissues such as heart and liver under concentrated impact loading (Kalcioglu et al., 2011).

Recently developed environmentally durable silicone gels, composed of a chemically crosslinked polydimethylsiloxane (PDMS) network loaded with a non-reactive PDMS solvent, offer the potential to mimic the complex mechanical response of soft biological tissues (Mrozek et al., 2011). By altering the concentration of elastically active crosslinking chains, trapped and untrapped physical chain entanglements, and dangling chain ends, as well as the corresponding molecular weight (MW) of these chains, both the elastic and viscoelastic properties of the silicone gels can be tuned systematically (Bibbo and Valles, 1984; Kawamura et al., 2002; Patel et al., 1992; Roth et al., 2004; Urayama, 2008; Vega et al., 2001; Villar and Valles, 1996). Thus, in addition to environmental stability, a significant advantage of silicone gels is the ability to tailor the properties by altering the network structure, solvent type, solvent loading, and solvent MW (Mrozek et al., 2011). Specifically, when the solvent MW is larger than the entanglement MW of the polymer, such PDMS-based gels can exhibit significant strain-rate stiffening, suggesting the potential to incorporate and tailor the strain rate-dependent response for tissue simulant applications. However, for this approach to be useful for the design of tissue simulants, such gels must be synthesized to match the approximate stiffness of most biological soft tissues, and the relevant mechanical response of interest – the extent and rate of energy dissipation under impact loading – must be compared directly between these organogels and the various hydrated biological tissues.

To that end, here we synthesized and analyzed the mechanical response of PDMS gels in comparison to tissues obtained from murine heart and liver. Due to the complexity of mechanical characterization at higher rates, rheological experiments at low strains and low shear rates were first conducted to provide insight into the effects of solvent loading, solvent MW, and network stochiometry on the frequency-dependent mechanical response as compared to the heart and liver tissues. Since such experiments cannot quantitatively predict the impact response of the materials, due to differences in loading rates and configurations as well as contact geometries (bulk sample response vs. local response in concentrated impact indentation), next we performed impact indentation experiments to quantify the impact resistance and the energy dissipation capacities and rates of these gels and tissues. These findings provide design principles and approaches to modulate the mechanical response of tissue simulant gels to concentrated impact loading, as required for the development of biofidelic tissue simulants.

2. Experimental

2.1 Materials

Gel processing details are discussed in previous work (Mrozek et al., 2011). These gels comprised a vinyl-terminated PDMS (v-PDMS; reactive network precursor) and methyl-terminated PDMS (m-PDMS; non-reactive theta solvent). Chain length of v-PDMS was 117 kg/mol, exceeding the entanglement molecular weight MW_{ENT} of PDMS (~29 kg/mol) (Gent et al., 1994) and leading to an entanglement-dominated network. We investigated gel properties by varying the solvent loading, solvent MW, and reaction stoichiometry (the molar ratio of silane to vinyl functional groups). The stoichiometry was varied from 4:1 (previously determined to provide an optimum network structure (Mrozek et al., 2011)) to 2:1. Solvent loading was varied from 10 vol% to 80 vol%, and the solvent MWs considered were 1.1, 139, and 308 kg/mol.

Heart and liver organs were harvested from adult rats. All experiments involving animals followed the University IACUC protocol and the NIH guidelines for animal care. Tissue discs of 8 mm-diameter and thickness of 3 to 5 mm were prepared using a surgical punch, and all tissues were stored in Krebs-Hensleit buffer immediately after excision and throughout all experiments reported herein.

2.2 Rheology

To measure the shear storage modulus *G'*, loss modulus *G"*, and loss tangent tan δ (i.e., *G"*/*G'* employed as a measure of the dissipation of deformation energy (Ferry, 1980)), rheological measurements on PDMS gels, heart and liver tissues were conducted. For details, see Supplementary Information S1.

2.3 Instrumented impact indentation

Impact indentation was conducted on all tissues and gels with a stainless steel flat punch probe of $R = 1$ mm at 25°C using a commercially available pendulum-based instrumented nanoindenter (Micro Materials Ltd., UK). Impact resistance described via maximum penetration depths $x_{\max}$, energy dissipation capacity K, and energy dissipation rate described via a quality factor Q were computed from the acquired displacement vs. time response of the pendulum. See Supplementary Information S2 for full discussion of this method and data analysis. Experiments herein were conducted at impact velocities ranging 0.4 - 2 cm/s, corresponding to a strain energy density of 2-20 kJ/m^3 comparable to other macroscale impact testing methods (Snedker et al., 2005) due to the relatively small probe contact area and volume.

3. Results & Discussion

3.1 Comparison of gel and tissue rheology at low strains and rates

3.1.1 Effect of solvent loading on the magnitude and rate dependence of G', G", and tan δ

Solvent has a significant impact on the modulus of these gels in two ways: (1) the solvent will dilute the polymer network to decrease the density of network chains per unit volume; and (2) the solvent will dilute the number of trapped entanglements. Both of these effects will be enhanced with increased solvent loading. Previous work with these silicone gels has shown that, at 50% solvent loading the low frequency *G'*, is ~ 40 kPa (Mrozek et al., 2011) which is stiffer than many biological soft tissues. Therefore, silicone gels of lower stiffness (greater mechanical compliance) are needed for tissue simulants that mimic soft tissue response. Thus, gels were synthesized to contain 10, 30, 40, 50, 60, 70, 75, 80, and 85 vol %

solvent using the optimum stoichiometry of 4:1 with a solvent MW of 1.1 kg/mol. Note that the optimum stoichiometry was determined by the reaction conditions that provided a maximum *G*'. The materials cured uniformly at solvent loadings up to 80 vol%; at 85 vol %, the gel consistency was not uniform and included significant volumes of uncured precursor. *G'* decreased as the solvent loading increased from 10% to 80% by approximately two orders of magnitude. Further, the lack of strong frequency-dependence in this measurement range was consistent with gels containing non-entangled solvents (Figure 1a). When *G'* measured at 1 Hz is graphed as a function of polymer vol% on a log-log scale, the data are well fit by a straight line, indicating power law behavior (Figure 1d). The obtained scaling factor (slope of the linear fit) of 2.5 is slightly larger than the theoretical value of 2.3 for a network formed in a theta solvent (Obukhov et al., 1994). *G"* also decreased by nearly two orders of magnitude when the solvent loading was increased from 10 to 80 vol% (Figure 1b). This resulted in a very low tan δ in the range of 0.07 to 0.005, consistent with low capacity for energy dissipation (Figure 1c). To provide a comparison, small-strain rheology was performed on murine heart and liver tissue (Supplementary Figure S2). The approximate mechanical response of these tissues is denoted in Figures 1a-c, and agree reasonably well with previous macroscale rheological experiments for liver (*G*' ~ 0.4 -10 kPa, and *G*" ~ 0.1 – 0.4 kPa) from various animal sources (Georges et al., 2007; Kiss et al., 2004; Liu and Bilston, 2000; Ozcan et al., 2011). These results show that although both the magnitude and frequency dependence of *G'* of heart were reasonably matched, we were unable to match the frequency dependence of *G"* by tuning the solvent loading %. Nevertheless, this comparison indicates that these gels can be tuned to exhibit macroscale storage moduli at low strains and strain rates that approximate those of biological soft tissues.

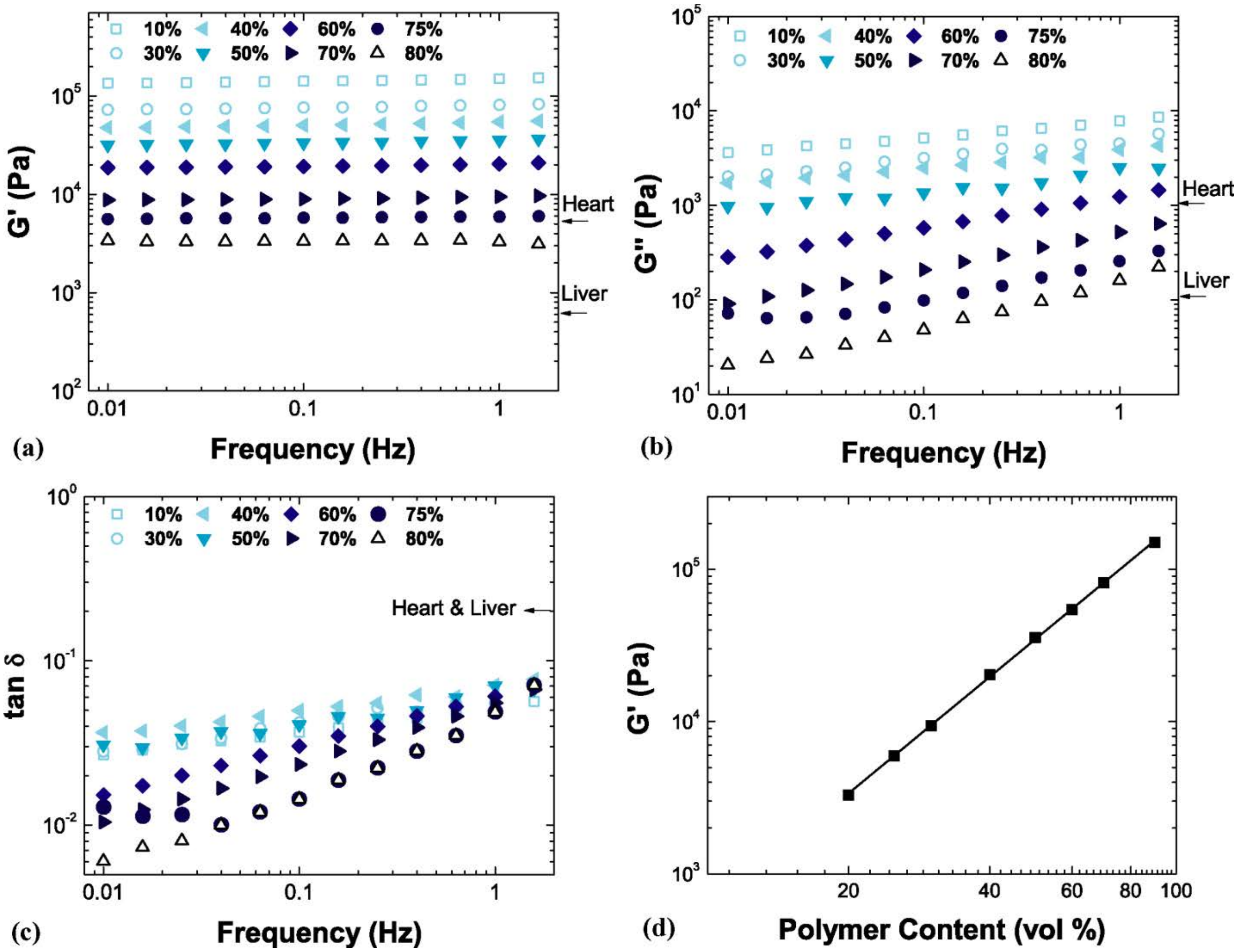

Figure 1. Effect of 1.1 kg/mol solvent loading: (a) storage modulus *G'*, (b) loss modulus *G"*, and (c) loss tangent tan *δ* with silane:vinyl stoichiometry of 4:1 as a function of frequency, compared to tissue from murine heart and liver. (d) *G'* as a function of polymer content for PDMS gels containing 1.1 kg/mol solvent.

3.1.2 Effect of solvent MW on the magnitude and rate dependence of G', G", and tan δ

Effects of solvent MW on the viscoelastic properties of the present gel system was investigated in detail previously (Mrozek et al., 2011). It was found that by manipulating the solvent MW to effectively modulate the number of entanglements per solvent chain, the gel mechanical response could be tuned. Gels were synthesized to comprise 10, 30, 40, 50, 60, 70, 75, and 80 vol% solvent, using the optimum stoichiometry 4:1 and a solvent MW of 308 kg/mol. Increasing the solvent MW from 1.1 kg/mol to 308 kg/mol did not significantly affect *G*' at low frequencies, indicating a consistent network microstructure (Figure 2a). However, higher solvent MW did induce an enhanced frequency dependence of *G*' (Figure 2a). The enhanced frequency-dependent *G*' is attributed to the longer relaxation times of the solvent chains in the polymer network as the solvent MW increases (Doi and Edwards, 1986; Gennes, 1979). Solvent chains are expected to enhance gel stiffness when the measurement time scale is shorter than the relaxation time of the solvent chains (Urayama et al., 2001), producing an increase in *G'* at higher frequencies. *G*" also increased significantly for solvent of higher MW, particularly at high solvent loadings (Figure 2b). This is attributed to the ability for the solvent to entangle with the network and with itself, providing mechanisms for energy dissipation. The enhanced energy dissipation results in much larger tan *δ* values at loadings above 50 vol % (Figure 2c). As a result, gels containing high MW solvent are too energy dissipative (larger tan δ) when compared to murine heart and liver tissue for gels that also exhibit the relevant range of storage moduli (i.e., solvent loadings of 70 to 80 vol %). To demonstrate that the solvent MW can be used to tailor the energy dissipation along with the strain-rate dependence, a gel was synthesized consisting of 75 vol % solvent using the optimum stoichiometry ratio and a solvent MW of 139 kg/mol (Figures 2d-f); this gel indeed exhibited a low-frequency *G*' similar to that of the gels containing 1.1 and 308 kg/mol (Figure 2d) and *G*" and tan *δ* that were intermediate to the higher and lower solvent MWs (Figures 2e-f).

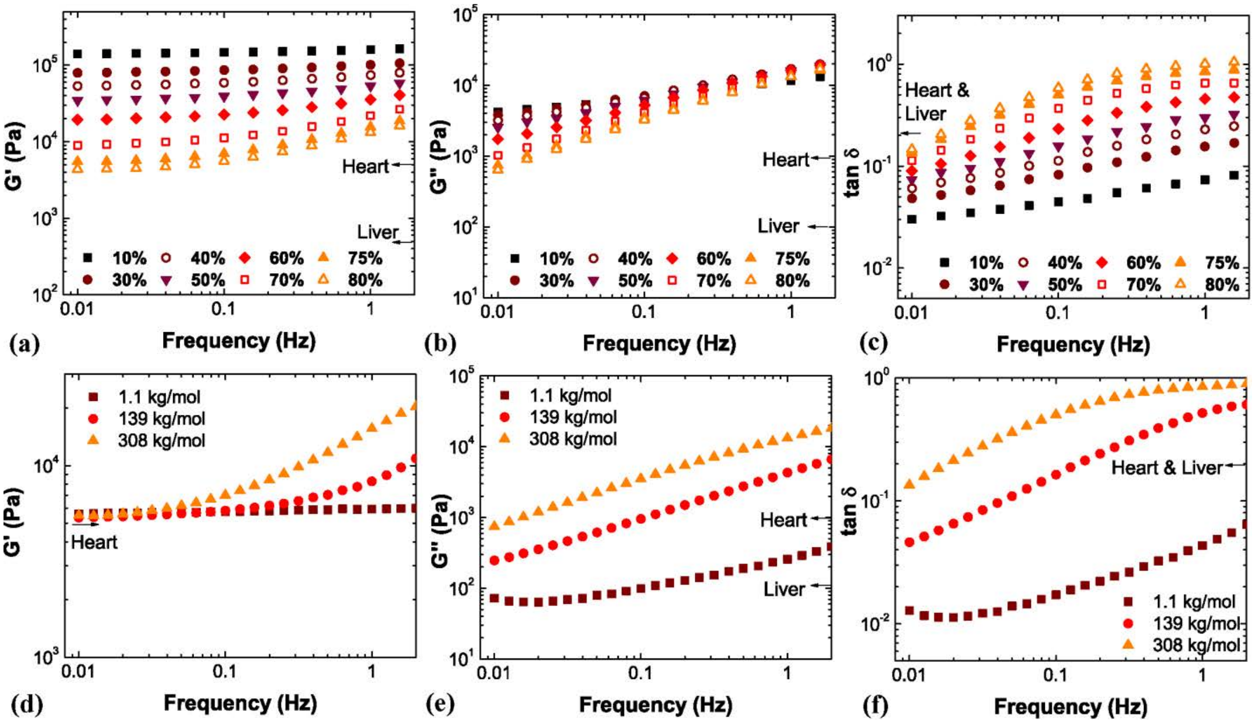

Figure 2. Effect of 308 kg/mol solvent loading: (a) storage modulus *G'*, (b) loss modulus *G"*, and (c) loss tangent tan δ values with silane:vinyl stoichiometry of 4:1 as a function of frequency, compared to heart and liver. Comparison of the (d) storage modulus *G'*, (e) loss modulus *G"*, and (f) loss tangent as a function of frequency for PDMS gels produced with a silane:vinyl stoichiometry of 4:1 containing 75 vol% solvent of 1.1, 139, and 308 kg/mol, resepectively.

3.1.3. Effect of stoichiometry on magnitude and rate dependence of G', G", and tan δ

The storage modulus of the gels can also be reduced through an increased incorporation of defects into the polymer network structure. Here, we examined gels at a range of crosslinker ratios (4:1 to 2.25:1) containing 60 vol% solvent with a MW of either 1.1 kg/mol or 308 kg/mol. Figure 3a shows that decreasing the stoichiometry (for the 1.1 kg/mol MW solvent gel) from 4:1 to 2.25:1 reduced *G*', particularly for silane to vinyl ratios less than 3:1. This correlated with decreased *G*' at low frequencies by nearly an order of magnitude, which was similar to the change in *G*' obtained by increasing the solvent loading from 60 to 80 vol% at a 4:1 stoichiometry (Figure 1a). Despite the decrease in *G*', *G"* did not change significantly as a function of stoichiometry (Figure 3b) leading to higher tan *δ* values for lower crosslinker ratios (Figure 3c). Similar to effects of solvent MW indicated in Figures 3a-c over a range of solvent loadings, here the solvent of higher MW resulted in enhanced frequency of *G*' and in increased *G*" and tan δ over a wide range of stoichiometric ratios (Supplementary Figure S3).

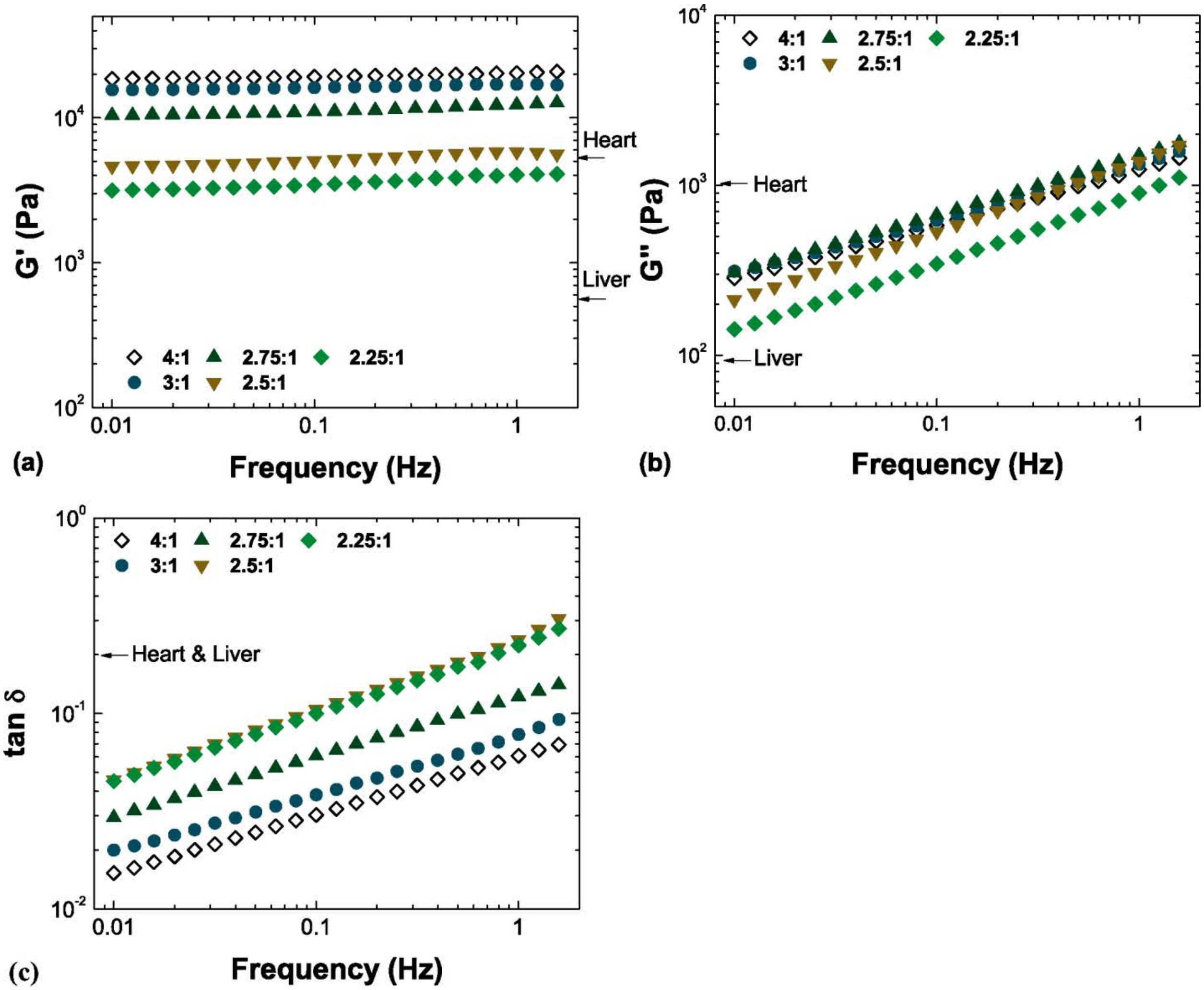

Figure 3. Effect of silane:vinyl stoichiometric ratio on (a) storage modulus *G'* and (b) loss modulus *G"*, (c) tan *δ* of of PDMS gels containing 60 vol% of 1.1 kg/mol solvent, compared to heart and liver tissues.

In summary, this rheological survey of a large library of PDMS gels indicates that the magnitude of *G*' can be tuned to match that of soft tissues at the frequencies studied herein, by decreasing the silane:vinyl stoichiometry and increasing the solvent loading. When the solvent MW was lower than the entanglement molecular weight (MW_{ENT}) of PDMS, changing the solvent loading or the stoichiometry did not alter the frequency dependence. By increasing the solvent MW to 308 kg/mol, gels were obtained that exhibited an increased frequency dependence. While matching the approximate stiffness and rate-dependent small strain response of biological tissues are important components of tissue simulant development, the impact resistance and energy dissipation processes at higher rates and larger strains are critical to recapitulate the response of soft tissues to abrupt, concentrated loading that is typical of intentional or accidental impact events.

3.2 Impact indentation experiments

3.2.1 Effect of solvent loading on x_{max}, K, and Q

Impact indentation experiments were conducted on heart and liver tissues and on PDMS gels with silane:vinyl stoichiometry of 4:1, solvent MW of 1.1 kg/mol, and a range of solvent loading including 60, 70, 75 and 80 vol%. As expected, $x_{\max}$ increased as the solvent loading increased (Figure 4a), indicating that the gels become less impact resistant with increasing solvent vol%. This is in agreement with small-strain rheology (Figure 1a), which showed decreased G' with increase in solvent loading. Representative stress vs. strain responses calculated at an impact velocity of ~0.7 cm/s also showed that the maximum forces attained decreased with increased solvent loading (Supplementary Figure S4a). Increased solvent loading also led to an increase in the impact velocity-dependence of penetration depths (Figure 4a) and in the energy dissipation capacity K (Figure 4b). Finally, energy dissipation was faster (lower Q) for higher solvent loadings (Figure 4c). Impact resistance of heart tissue was matched most closely by the gel comprising 70 vol% solvent. However, this gel dissipated less energy in the first impact event (lower K) and dissipated this energy more slowly (higher Q) than both heart and liver tissues under the impact velocities considered. Although the gel comprising 80 vol% solvent most closely approached the impact resistance, K, and Q of liver tissue, all of these gels were in fact more impact resistant and exhibited lower capacities and rates of energy dissipation than liver tissue. Thus, although trends as a function of solvent loading are clear, modulation of only this parameter is insufficient to mimic the impact behavior of either of these soft tissues.

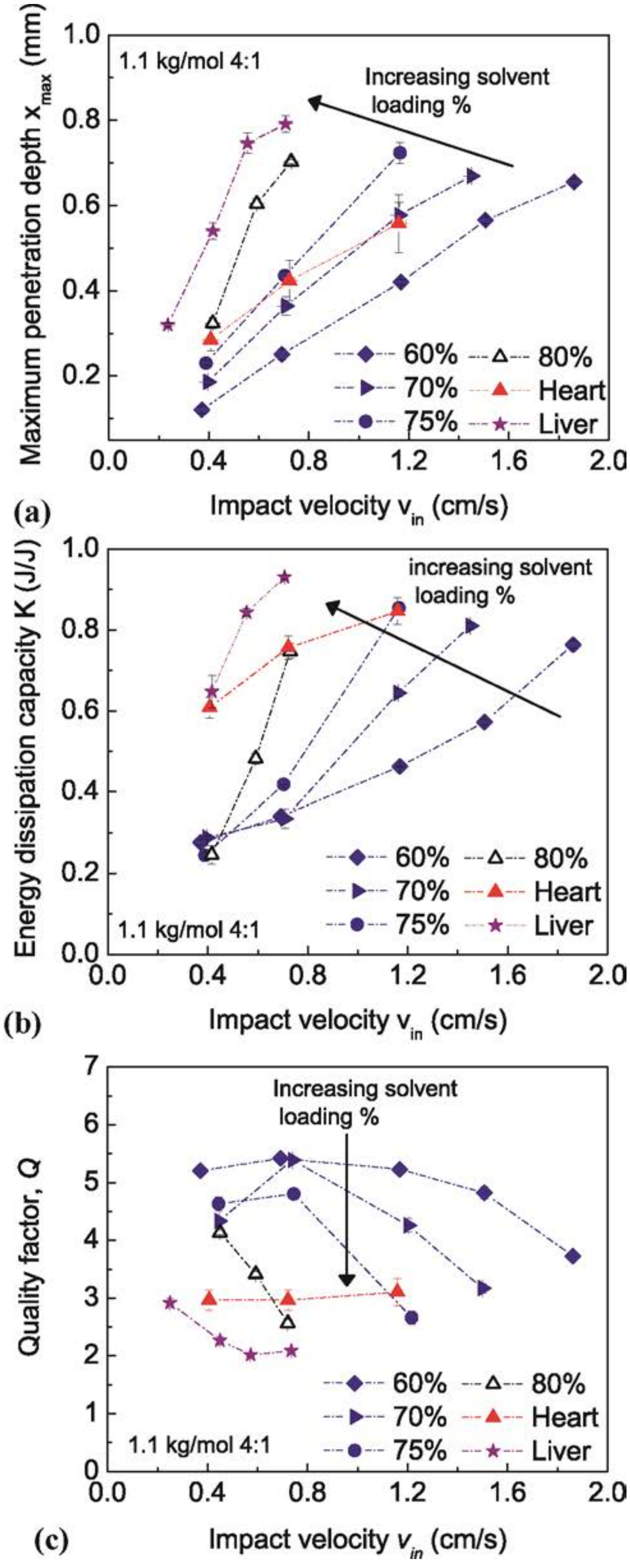

Figure 4. Effect of solvent loading % for PDMS gels with silane:vinyl stoichiometric ratio of 4:1 and solvent molecular weight of 1.1 kg/mol (a) Maximum penetration depth $x_{\max}$ as a function of impact velocity: as the solvent loading % increases, the gels become less impact resistant; this effect is more pronounced at higher impact velocities. (b) Energy dissipation capacity K as a function of impact velocity: K increases as solvent loading % increases; this effect is more pronounced at higher impact velocities.(c) Quality factor Q as a function of impact velocity: increasing the solvent loading% decreases Q (i.e., increases the energy dissipation rate). Data are represented as mean ± standard error, and standard error bars may appear smaller than the symbols.

3.2.2 Effect of solvent MW on x_{max}, K, and Q

Impact indentation experiments were conducted on PDMS gels with solvent loading of 80 vol% and silane:vinyl stoichiometric ratio of 4:1 for solvent MWs of 1.1, 139 and 308 kg/mol. Figure 5a shows that impact resistance of these gels increased with increasing MW of the solvent (lower $x_{\max}$). Further, the dependence of $x_{\max}$ on impact velocity was enhanced with decreasing solvent MW. This suggests that the rate of stiffening of the gels decreased as the solvent MW decreased, recalling the macroscale rheological trends of decreased frequency dependence of storage moduli with decreasing solvent MW. Such increased stiffness and impact resistance are consistent with the concept of an increased number of physical entanglements as the solvent MW surpasses MW_{ENT}. Energy dissipation capacity (Figure 5b) and rate (Figure 5c) also increased substantially as the solvent MW surpassed MW_{ENT}, which could be attributed to increased physical entanglements and to correspondingly decreased solvent mobility. In fact, gels of solvent MWs of 139 kg/mol and 308 kg/mol dissipated most or all of the energy during the first impact leading to $K{\sim}1$ and Q less than unity (dashed line). We note that, although adhesion was mitigated to the extent possible in these experiments, gel adhesion to the impact probe surface was qualitatively greater at higher solvent MWs; this could serve as an additional mechanism for energy dissipation. We conclude from these results that gels comprising solvents of lower MW are favored candidates to approximate the impact response of heart and liver tissues.

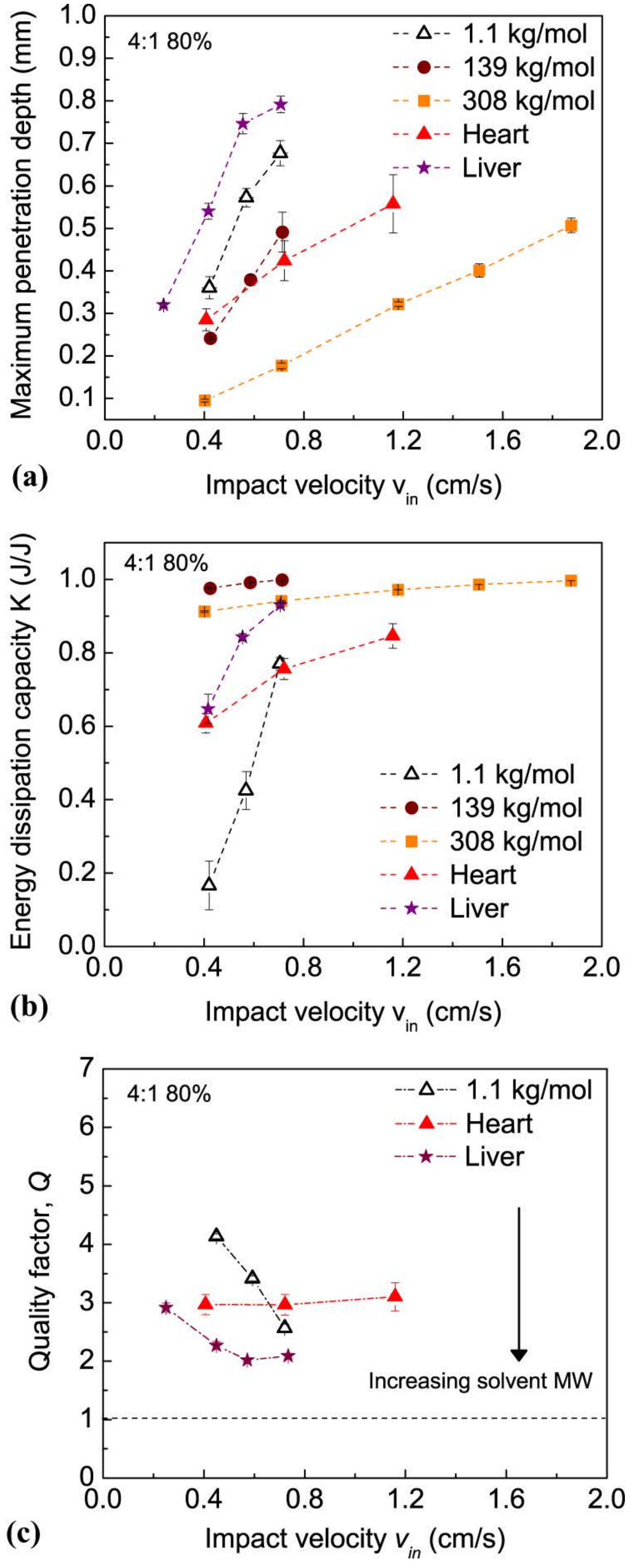
4:1 80%
1.1 kg/mol
139 kg/mol
308 kg/mol
Heart
Liver
Maximum penetration depth (mm)
1.0
0.9
0.8
0.7
0.6
0.5
0.4
0.3
0.2
0.1
0.0
0.4
0.8
1.2
1.6
2.0
(a)
Impact velocity v_{in} (cm/s)
4:1 80%
Energy dissipation capacity K (J/J)
1.0
0.8
0.6
0.4
0.2
0.0
1.1 kg/mol
139 kg/mol
308 kg/mol
Heart
Liver
0.0
0.4
0.8
1.2
1.6
2.0
(b)
Impact velocity v_{in} (cm/s)
4:1 80%
1.1 kg/mol
Heart
Liver
Quality factor, Q
7
6
5
4
3
2
1
0
Increasing solvent MW
0.0
0.4
0.8
1.2
1.6
2.0
(c)
Impact velocity v_{in} (cm/s)

Figure 5. Effect of solvent molecular weight on impact response of PDMS gels with a 4:1 precursor chain stoichiometry and 80 vol% solvent loading: (a) Maximum penetration depths as a function of impact velocity: gels become more impact resistant as the molecular weight (MW) of the solvent increases; this effect is more pronounced at higher impact velocities. (b) Energy dissipation capacity *K* as a function of solvent MW: gels of larger solvent MW are more dissipative at a given impact velocity. (c) Quality factor *Q* as a function of impact velocity: increasing solvent MW increases the energy dissipation rate (lower *Q*), to the extent that for gels with MW>1.1 kg/mol, energy was dissipated during the first impact cycle leading to *Q* values below the dashed line. Data are represented as mean ± standard error.

3.2.3 Effect of stoichiometry on $x_{max,}$ K, and Q

To investigate the effect of precursor chain stoichiometry (representing the crosslink density within the present range) on impact responses, PDMS gels loaded with solvent of 1.1 kg/mol MW at 60 vol% were considered; stoichiometric ratios ranged from 2:1 to 4:1. Figure 6a shows that impact resistance of these gels increased for a given impact velocity as the crosslinking density increased (i.e., as stoichiometry varied from 2:1 to 4:1). These trends agreed well with macroscale rheology, for which increasing crosslinking density resulted in increased *G*' (Figure 3a). Representative stress vs. strain responses calculated at an impact velocity of ~0.7 cm/s also showed that maximum attainable forces increased with increased crosslinking density (Supplementary Figure S4b). Gels of highest crosslinking densities (3:1 and 4:1 ratio) exhibited similar x_{max}, indicating that further increases in crosslinker density would be unlikely to further decrease x_{max} because the mechanical response is already entanglement dominated; the stoichiometric ratio was already optimal at 4:1 (Mrozek et al., 2011). Increasing the amount of crosslinker resulted in lower energy dissipation capacities (lower *K*, Figure 6b) and lower energy dissipation rates (higher *Q*, Figure 6c), due ostensibly to an increase in the elastic chains and a decrease in the incorporation of dangling chain ends. Impact resistance and energy dissipation rate of heart tissue were best matched by gels comprising 60 vol% of 1.1 kg/mol solvent at a precursor stoichiometric ratio of

2.75:1. Impact resistance of liver tissue was best matched by gels comprising 60 vol% of 1.1 kg/mol solvent at a precursor stoichiometric ratio of 2:1, though this candidate tissue simulant dissipated more energy than liver tissue (higher K).

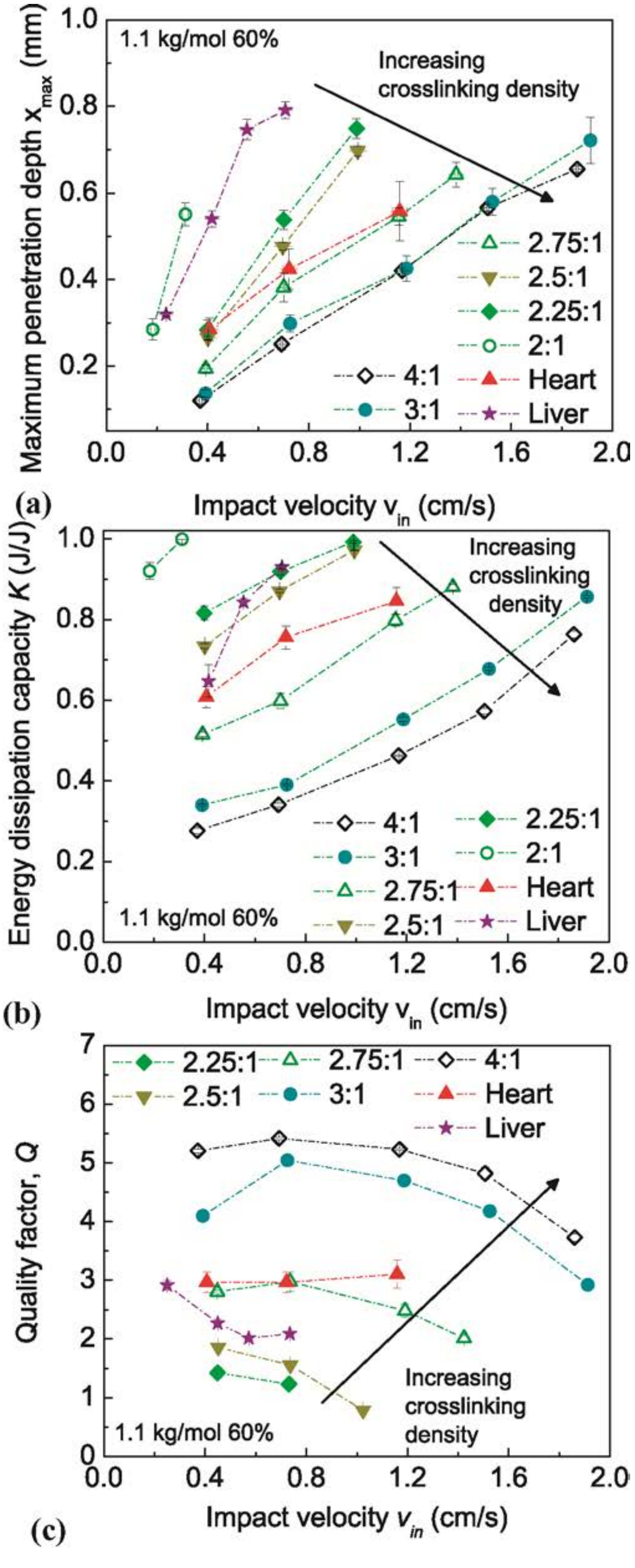

1.1 kg/mol 60%
Increasing crosslinking density
Maximum penetration depth x_{max} (mm)
1.0
0.8
0.6
0.4
0.2
0.0
0.4
0.8
1.2
1.6
2.0
2.75:1
2.5:1
2.25:1
2:1
4:1
3:1
Heart
Liver
(a)
Impact velocity v_{in} (cm/s)
Energy dissipation capacity K (J/J)
1.0
0.8
0.6
0.4
0.2
0.0
Increasing crosslinking density
4:1
3:1
2.75:1
2.5:1
2.25:1
2:1
Heart
Liver
1.1 kg/mol 60%
0.0
0.4
0.8
1.2
1.6
2.0
Impact velocity v_{in} (cm/s)
(b)
7
6
5
4
3
2
1
0
2.25:1
2.75:1
4:1
2.5:1
3:1
Heart
Liver
Quality factor, Q
Increasing crosslinking density
1.1 kg/mol 60%
0.0
0.4
0.8
1.2
1.6
2.0
Impact velocity v_{in} (cm/s)
(c)

Figure 6. Effect of silane:vinyl stoichiometric ratio for PDMS gels with 60 vol% 1.1 kg/mol molecular weight solvent (a) Maximum penetration depths as a function of impact velocity: impact resistance of gels increases (lower $x_{\max}$) by increasing the crosslink density; this effect is more pronounced at higher impact velocities. Impact resistance of heart and liver tissues is matched by the PDMS gels. (b) Energy dissipation capacity K as a function of impact velocity: gels dissipate more energy at lower crosslinking densities. Energy dissipation capacity of the tissues is matched by the gels with lower crosslinking. (c) Quality factor Q as a function of impact velocity: gels dissipate energy more quickly (lower Q) as the crosslinking density decreases. Both heart and liver show comparable energy dissipation rates to the gels with lower crosslinking density. Data are represented as mean ± standard error, and error bars may appear smaller than data symbols.

3.2.4 Comparison of impact response among gels and soft tissues

The above discussion makes clear that the three design parameters considered (solvent vol%, solvent MW, and precursor ratio) can result in coupled or competing effects on the impact performance metrics of interest ($x_{\max}$, K, and Q). Quantification and understanding of this coupling allows us to move from many iterative experiments to reasonably predictive design of impact performance. Here, we demonstrate the tuning of these "knobs" to realize a tissue simulant for heart tissue impact response, and discuss how these same principles can be extended toward design of mechanical tissue simulants for other, more compliant tissues such as liver.

Heart - Our impact indentation experiments showed that two gels exhibited similar impact resistance (i.e., $x_{\max}$) to that of heart tissue for the impact velocities studied here (Figure 7a). These gels comprised solvent of 1.1 kg/mol MW, with loading/precursor chain stoichiometry of 70 vol%/4:1 or 60 vol%/2.75:1. In these gel families, we observed that impact resistance could be tuned by opposing design parameters: increasing the solvent loading from 60 vol% to 70 vol% increased $x_{\max}$, and increasing the crosslinking density (changing the stoichiometry from 2.75:1 to 4:1) decreased $x_{\max}$. Although these two gels exhibited similar impact resistance, the candidate with the lower solvent loading and crosslinking density dissipated more energy during the first impact event (larger K), and dissipated this energy more quickly (lower Q) (Figures 7b,c). Thus, this tissue simulant candidate better matches the impact response of heart tissue in terms of the magnitudes of $x_{\max}$, K, and Q, and the impact velocity-dependence of $x_{\max}$ and K. More importantly, by tuning the crosslinker density and solvent loading, we individually tuned the three metrics of impact behavior to better mimic the response of a specific biological tissue. Finally, although this gel exhibited a slight decrease in the magnitude of Q at higher impact velocities, Q of heart did not depend on impact velocity for the velocities explored herein. Based on our findings, one could speculate that by decreasing the solvent loading vol% to below 60%, the velocity-dependence of Q in these gels would decrease (Figure 4c), and better match that of heart tissue. However, this change would also lead to an increase in the magnitude of Q, and a decrease in the magnitude and velocity-dependence of x_{max} and K, resulting in a mismatch of those parameters. To compensate for this outcome, the silane:vinyl stoichiometric ratio may be slightly decreased to below 2.75:1, which would cause an increase in the magnitude of x_{max} and K, a decrease in the magnitude of Q, and an increase in the velocity dependence of x_{max} without significantly affecting the velocity dependence of Q (Figure 6).

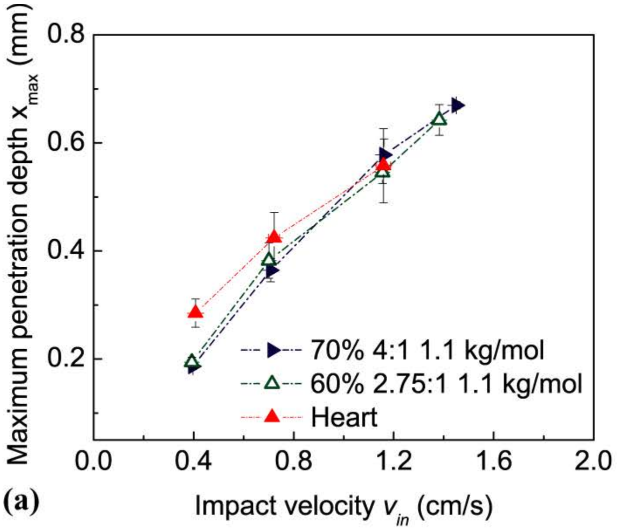
Maximum penetration depth x_{max} (mm)
0.8
0.6
0.4
0.2
0.0
0.4
0.8
1.2
1.6
2.0
Impact velocity v_{in} (cm/s)
70% 4:1 1.1 kg/mol
60% 2.75:1 1.1 kg/mol
Heart

(a)

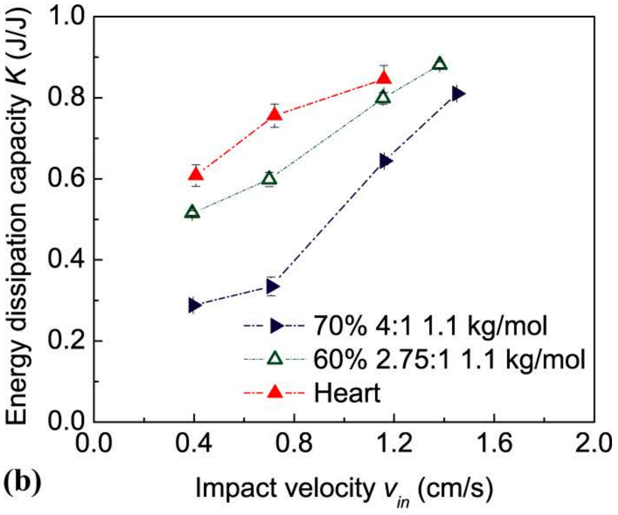
Energy dissipation capacity K (J/J)
1.0
0.8
0.6
0.4
0.2
0.0
0.0
0.4
0.8
1.2
1.6
2.0
Impact velocity v_{in} (cm/s)
70% 4:1 1.1 kg/mol
60% 2.75:1 1.1 kg/mol
Heart

(b)

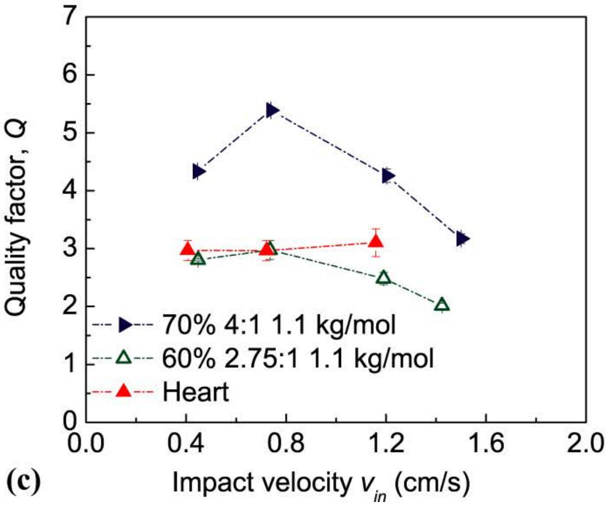
Quality factor, Q
7
6
5
4
3
2
1
0
0.0
0.4
0.8
1.2
1.6
2.0
Impact velocity v_{in} (cm/s)
70% 4:1 1.1 kg/mol
60% 2.75:1 1.1 kg/mol
Heart

(c)

Figure 7. (a) By changing the solvent loading vol% and silane:vinyl stoichiometry, we compare two different gels that both mimic the impact resistance of heart tissue for the impact velocities explored herein. (b) These two gel systems exhibit distinct energy dissipation capacities K (b) and quality factor Q (c). For the impact velocities considered, the gel with 60 vol% solvent of 1.1 kg/mol MW and silane:vinyl stoichiometry of 2.75:1 most closely mimics heart tissue by all three metrics of mechanical impact response.

Liver - We identified several gels that exhibited either $x_{\max}$ (Figure 8a), K (Figure 8b), or Q (Figure 8c) that were similar to those of liver tissue for the impact velocities studied here. However, unlike for the case of heart tissue, none of these gels captured the magnitude and velocity-dependence of impact response of liver tissue by all metrics. For example, gels with a composition of 80 vol%-4:1-1.1 kg/mol and 60 vol%-2:1-1.1 kg/mol exhibited $x_{\max}$ similar to liver tissue, while the former dissipated less energy and the latter dissipated more energy than liver. Further increasing the MW of the 80% 4:1 gel from 1.1 to 139 kg/mol increased the magnitude of K but also decreased the magnitude of $x_{\max}$ and velocity-dependence of K significantly. On the other hand, gel systems with a composition of 60 vol%-2.5:1-1.1 kg/mol and 60 vol%-2.25:1-1.1 kg/mol exhibited similar magnitude of K values to liver but yielded lower magnitude of $x_{\max}$ and a decrease in the impact velocity-dependence of K. Although it is beyond the scope of the current study to further optimize these gels toward liver tissue simulants, we can draw on the design parameters identified above to now suggest further iterations toward that aim. Based on the gels considered herein, an improved liver tissue simulant could plausibly be attained by increasing the solvent vol% in gels with low crosslinking density (between 60% to 70% for 2.25:1 or 2.5:1 gels); this tuning would be expected to increase the magnitude of $x_{\max}$ and the velocity dependence of $x_{\max}$ and K. However, this increase in the solvent vol% would also likely increase the magnitude of K values to be higher and decrease the magnitude of Q values to be lower than that of liver. To compensate for this change, crosslinking density could be increased only slightly (precursor ratios between 2.5:1 and 2.75:1) to achieve lower K and higher Q values without significantly altering the magnitude of x_{max} and the velocity-dependence of K, Q, and x_{max}.

In summary, we identified design principles required to simultaneously optimize key metrics of impact response for PDMS-based gels. We thus demonstrated specific gel compositions that matched the impact response of heart tissue with reasonable fidelity. These findings inform the design of synthetic gels to recapitulate the response of specific biological materials under impact.

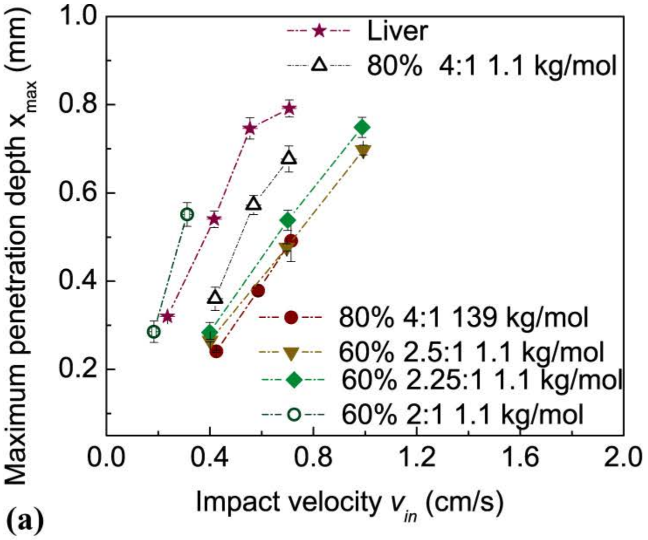
Maximum penetration depth x$_{max}$ (mm)
1.0
0.8
0.6
0.4
0.2
0.0
0.4
0.8
1.2
1.6
2.0
Impact velocity v_{in} (cm/s)
Liver
80% 4:1 1.1 kg/mol
80% 4:1 139 kg/mol
60% 2.5:1 1.1 kg/mol
60% 2.25:1 1.1 kg/mol
60% 2:1 1.1 kg/mol

(a)

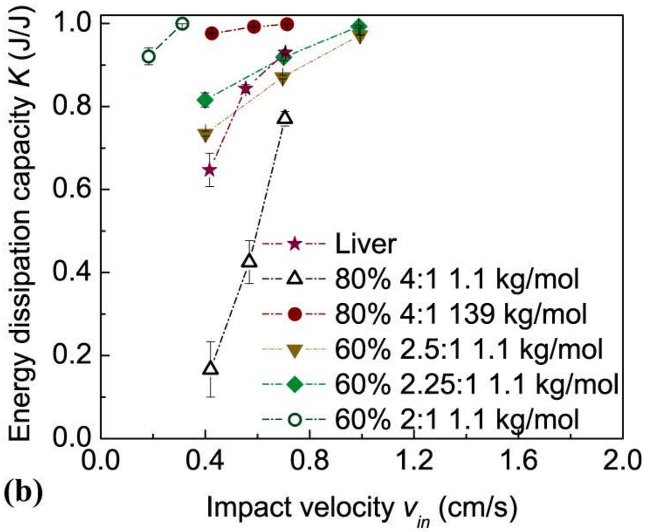
Energy dissipation capacity K (J/J)
1.0
0.8
0.6
0.4
0.2
0.0
0.0
0.4
0.8
1.2
1.6
2.0
Impact velocity v_{in} (cm/s)
Liver
80% 4:1 1.1 kg/mol
80% 4:1 139 kg/mol
60% 2.5:1 1.1 kg/mol
60% 2.25:1 1.1 kg/mol
60% 2:1 1.1 kg/mol

(b)

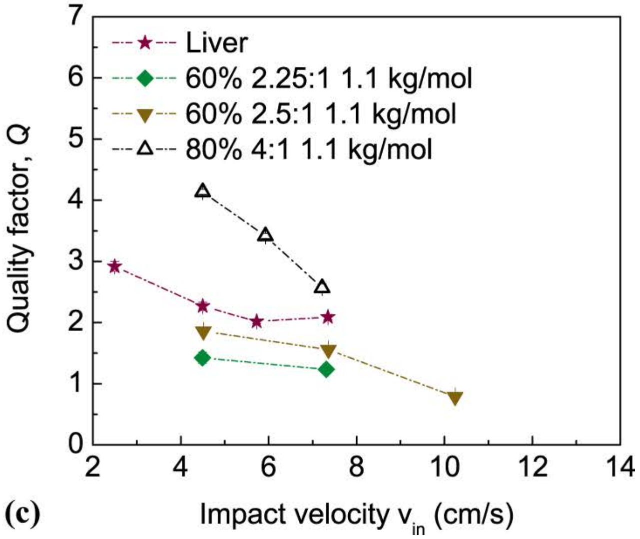
Quality factor, Q
7
6
5
4
3
2
1
0
2
4
6
8
10
12
14
Impact velocity v$_{in}$ (cm/s)
Liver
60% 2.25:1 1.1 kg/mol
60% 2.5:1 1.1 kg/mol
80% 4:1 1.1 kg/mol

(c)

Figure 8. (a) The two top candidates for matching liver tissue impact resistance are the PDMS gels with 60 vol% solvent/silane:vinyl stoichiometry of 2:1, and 80 vol% solvent/silane:vinyl stoichiometry of 4:1, both with solvent MW of 1.1 kg/mol. The two top candidates for matching energy dissipation capacity *K* (b) and quality factor *Q* (c) of liver tissue are the PDMS gels with 60 vol% solvent/silane:vinyl stoichiometry of 2.25:1, and 60 vol% solvent/silane:vinyl stoichiometry of 2.5:1, both with solvent MW of 1.1 kg/mol.

Conflict of interests

The authors do not have any conflict of interest.

Acknowledgments

This research was supported in part by the U.S. Army through the Institute for Soldier Nanotechnologies, under Contract W911NF-07-D-0004 with the U.S. Army Research Office. Certain commercial equipment and materials are identified in this paper in order to specify adequately the experimental procedure. In no case does such identification imply recommendations by the Army Research Laboratory nor does it imply that the material or equipment identified is necessarily the best available for this purpose.

References

Appleby-Thomas, G.J., Hazell, P.J., Wilgeroth, J.M., Shepherd, C.J., Wood, D.C., Roberts, A., 2011. On the dynamic behavior of three readily available soft tissue simulants. Journal of Applied Physics 109, 084701.

Bertrand, S., Cuny, S., P, P.P., Trosseille, X., Page, Y., Guillemot, H., Drazetic, P., 2008. Traumatic rupture of thoracic aorta in real-world motor vehicle crashes. Journal of Traffic Injury Prevention 9, 153-161.

Bibbo, M.A., Valles, E.M., 1984. Influence of pendant chains on the loss modulus of model networks. Macromolecules 17, 360-365.

Bisplinghoff, J., McNally, C., Manoogian, S., Duma, S., 2009. Dynamic material properties of the human sclera. Journal of Biomechanics 42, 1493-1497.

Bresson, F., Frank, O., 2010. Comparing ballistic wounds with experiments on body simulator. Forensic Science International 193, e23-27.

Constantinides, G., Tweedie, C.A., Savva, N., Smith, J.F., VanVliet, K.J., 2009. Quantitative Impact Testing of Energy Dissipation at Surfaces. Experimental Mechanics 49, 511-522.

Constantinidies, G., Tweedie, C.A., Holbrook, D.M., Barragan, P., Smith, J.F., VanVliet, K.J., 2008. Quantifying deformation and energy dissipation of polymeric surfaces under localized impact. Materials Science and Engineering A 489, 403-412.

Doi, M., Edwards, S.F., 1986. The theory of Polymer dynamics. Clarendon Press, Oxford, UK.

Ferry, J.D., 1980. Viscoelastic Properties of Polymers. John Wiley & Sons, New York.

Gennes, P.-G., 1979. Scaling concepts in polymer physics. Cornell University Press, Ithaca, NY.

Gent, A.N., Liu, G.L., Mazurek, M.J., 1994. Experimental study of molecular entanglement in polymer networks. Journal of Polymer Science Part B: Polymer Physics 32, 271-279.

Georges, P.C., Hui, J.-J., Gombos, Z., McCormick, M.E., Wang, A.Y., Uemura, M., Mick, R., Janmey, P.A., Furth, E.E., Wells, R.G., 2007. Increased stiffness of the rat liver precedes matrix deposition: implications for fibrosis. American Journal of Physiology - Gastrointestinal and Liver Physiology 293, G1147–G1154.

Gong, J., 2010. Why are double network hydrogels so tough? Soft Matter 6, 2583-2590.

Juliano, T.F., Foster, A.M., Drzal, P.L., Weesooriya, T., Moy, P., VanLandingham, M.R., 2006. Multiscale Mechanical Characterization of Biomimetic Physically Associating Gels. Journal of Materials Research 21, 2084-2092.

Jussila, J., Leppaniemi, A., M, M.P., Kulomaki, E., 2005. Ballistic skin simulant. Forensic Science International 150, 63-71.

Kalcioglu, Z.I., Qu, M., Strawhecker, K.E., Shazly, T., Edelman, E., VanLandingham, M.R., Smith, J.F., VanVliet, K.J., 2011. Dynamic impact indentation of hydrated biological tissues and tissue surrogate gels. Philosophical Magazine 91, 1339–1355.

Kawamura, T., Urayama, K., Kohjiya, S., 2002. Multiaxial Deformations of End-Linked Poly(dimethylsiloxane) Networks. III. Effect of Entanglement Density on Strain-Energy Density Function. Journal of Polymer Science Part B: Polymer Physics 40, 2780-2790.

Kiss, M.Z., Varghese, T., Hall, T.J., 2004. Viscoelastic characterization of in vitro canine tissue. Physics in Medicine and Biology 49, 4207–4218.

Lenhart, J., Cole, P., 2006. Adhesion Properties of Lightly Crosslinked Solvent-Swollen Polymer Gels. Journal of Adhesion 82, 945-971.

Liu, Z., Bilston, L., 2000. On the viscoelastic character of liver tissue: Experiments and modeling of the linear behavior. Biorheology 37, 91–201.

Merkle, A., Ward, E., O'Connor, J., Roberts, J., 2008. Assessing behind armor blunt trauma (BABT) under NIJ standard-0101.04 conditions using human torso models. Journal of Trauma-Injury Infections and Critical Care 64, 1555-1561.

Moy, P., Weerasooriya, T., Juliano, T.F., VanLandingham, M.R., 2006. Dynamic Response of an Alternative Tissue Simulant, Physically Associating Gels (PAG). In Proceedings of the Society for Experimental Mechanics Conference. St. Louis, Missouri.

Mrozek, R., Knorr, D., Spangler, S., Cole, P., Lenhart, J., 2012. Impact of precursor size on the chain structure and mechanical properties of solvent swollen epoxy gels. Soft Matter doi:10.1039/c2sm25768h

Mrozek, R.A., Cole, P.J., Otim, K.J., Shull, K.R., Lenhart, J.L., 2011. Influence of solvent size on the mechanical properties and rheology of polydimethylsiloxane-based polymeric gels. Polymer 52, 3422-3430

Nicolle, S., Vezin, P., Parlierne, J.-F., 2010. A strain hardening bi-power law for the nonlinear behavior of biological soft tissues. Journal of Biomechanics 43, 927-932.

Obukhov, S.P., Rubinstein, M., Colby, R.H., 1994. Network modulus and superelasticity Macromolecules 27, 3191-3198.

Oliver, M., Kovats, T., Mijailovich, S., Butler, J., Fredberg, J., Lenormand, G., 2010. Remodeling of integrated contractile tissues and its dependence on strain-rate amplitude. Physical Review Letters 105, 158102

Ozcan, M.U., Ocal, S., Basdogan, C., Dogusoy, G., Tokat, Y., 2011. Characterization of frequencydependent material properties of human liver and its pathologies using an impact hammer. Medical Image Analysis 15, 45-52.

Patel, S.K., Malone, S., Cohen, C., Gillmot, J.R., Colby, R.H., 1992. Elastic Modulus and Equilibrium Swelling of Poly(dimethylsiloxane) Networks. Macromolecules 25, 5241-5251.

Roberts, J., Merkle, A., Biermann, P., Ward, E., Carkhuff, B., Cain, R., OConnor, J., 2007. Computational and experimental models of the human torso for non-penetrating ballistic impact Journal of Biomechanics 40, 125-136.

Roth, L.E., Vega, D.A., Valles, E.M., Villar, M.A., 2004. Viscoelastic properties of networks with low concentration of pendant chains. Polymer 45, 5923-5931.

Saraf, H., Ramesh, K., Lennon, A., Merkle, A., Roberts, J., 2007. Mechanical properties of soft human tissues under dynamic loading. Journal of Biomechanics 40, 1960-1967.

Seitz, M., Martina, D., Baumberger, T., Krishnan, V., KR, K.S., 2009. Fracture and large strain behavior of self-assembled triblock copolymer gels. Soft Matter 5, 447-456.

Snedker, J., Barbezat, M., Niederer, P., Scmidlin, F., Farshad, M., 2005. Strain energy density as a rupture criterion for the kidney: impact tests on porcine organs, finite element simulation, and a baseline comparison between human and porcine tissues. Journal of Biomechanics 38, 993-1001.

Song, B., Chen, W., Ge, Y., Weerasooriya, T., 2007. Dynamic and quasi-static compressive response of porcine muscle. Journal of Biomechanics 40, 2999-3005,.

Stammen, J., Williams, S., Ku, D., Guldberg, R., 2001. Mechanical Properties of a novel PVA hydrogel in shear and unconfined compression. Biomaterials 22, 799-806.

Storm, C., Pastore, J., MacKintosh, F., Lubensky, T., Janmey, P., 2005. Nonlinear elasticity in biological gels. Nature 435, 191-194.

Thali, M., Kneubuehl, B., Zollinger, U., Dirnhofer, R., 2002. The skin-skull-brain model: a new instrument for the study of gunshot effects. Forensic Science International 125, 178-189.

Urayama, K., 2008. Network Topology–Mechanical Properties Relationships of Model Elastomers. Polymer Journal 40, 669–678.

Urayama, K., Yokoyama, K., Kohjiya, S., 2001. Viscoelastic Relaxation of Guest Linear Poly(dimethylsiloxane) in End-Linked Poly(dimethylsiloxane) Networks. Macromolecules 34, 4513-4518.

Vega, D.A., Villar, M.A., Alessandrini, J.L., Valles, E.M., 2001. Terminal Relaxation of Model Poly(dimethylsiloxane) Networks with Pendant Chains. Macromolecules 34, 4591-4596.

Villar, M.A., Valles, E.M., 1996. Influence of Pendant Chains on Mechanical Properties of Model Poly(dimethylsiloxane) Networks. 2. Viscoelastic Properties. Macromolecules 29, 4081-4089.

Weiss, J., Gardiner, J., Bonifasi-Lista, C., 2002. Ligament material behavior is nonlinear, viscoelastic rate-independent under shear loading. Journal of Biomechanics 35, 943-950.

Supplementary Information and Figures

S1. Rheology

Rheological experiments on PDMS gels were conducted adopting a torsion geometry (MCR 501, Anton Paar, Austria) at 25^{o}C using rectangular samples of approximately 12 ×4.5 × 28 mm. Frequency-dependent data were measured at 1% shear strain remaining within the linear viscoelastic regime at a range of 0.01 - 2 Hz (n = 3-5 replicate on each sample). Data are reported as the median of replicate experiments on the same sample with an error of less than 5%.

Oscillatory shear rheological measurements of heart and liver tissues (n=3 for each tissue source) were conducted in a parallel plate geometry at 37^{o}C (MCR 501, Anton Paar, Austria) within 5 h post mortem. Tissues were adhered to the bottom plate using a thin layer of cyanoacrylate and a profiled top plate was utilized to ensure a secure grip on the sample. Frequency-dependent modulus data were measured in a frequency range of 0.1 - 10 Hz at 1% strain. Tissue measurements were not extended to lower frequencies to avoid dehydration over extended experimentation time scales. Data are reported as the mean of replicate experiments on samples from unique animal donors with a standard deviation of less than 30%.

S2. Impact indentation experiments

The instrument was modified previously and calibrated to enable impact indentation of compliant and adhesive materials in fully hydrated conditions (Constantinides et al., 2009; Constantinidies et al., 2008; Kalcioglu et al., 2011). Heart and liver tissues were harvested from three different animals and tested within 3 h post mortem. For the impact indentation experiments, probe displacement was recorded throughout successive impact cycles until the probe came to rest (Figure S1a). Impact resistance was quantified by the maximum penetration depth x_{max}. Energy dissipation capacity K was calculated as the energy dissipated by the sample normalized by corresponding total energy (sum of dissipated and recovered sample energies) in the first impact event. The rate of energy dissipation was described via a quality factor Q that is related to the number of cycles or time required to dissipate the impact. Pendulum motion was described as damped harmonic oscillation, and an exponentially decaying function was fitted to the maxima of probe displacement vs. time (dashed line, Figure S1b). Q was calculated accordingly as the time required for the oscillation amplitude to decay by a factor of $1/e$. With this definition, larger Q values corresponded to lower energy dissipation rates. Full details on derivation of energy dissipation parameters have been described previously (Constantinides et al., 2009; Constantinidies et al., 2008; Kalcioglu et al., 2011). Replicate experiments were conducted at each impact velocity for both gels (n=3) and tissues (n=5). Data are reported as mean ± standard error of measurement.

Although these experiments are not designed specifically to extract stress vs. strain responses with high accuracy, for completeness we note that stress was estimated from the resistive force of the material F_m:

$$F_\mathrm{m} = F_\mathrm{acc} - ma \tag{S.1}$$

where F_acc is the accelerating force applied on the indenter, m is the mass (0.17 kg), and a is the acceleration of the pendulum calculated from pendulum displacement over time. Stress was calculated as $F_\mathrm{m} /(\pi R^2)$, where R is the radius of the cylindrical probe. Applied strains were estimated as the ratio h/R where h is the displacement of the indenter. Due to the comparatively high adhesivity of these gels, PDMS gels were immersed in an aqueous solution containing 3% Pluronic® F108 during mechanical characterization. This enabled quantification of gel impact response with minimized adhesive interactions between this specific probe and the sample surfaces; future studies could be undertaken to compare energy dissipation as a function of probe material. Separate paired experiments were conducted in air and fluid to verify negligibility of the contribution of fluid drag forces to the overall damping of the system, and ensure that testing in fluid did not affect the measured properties of the samples.

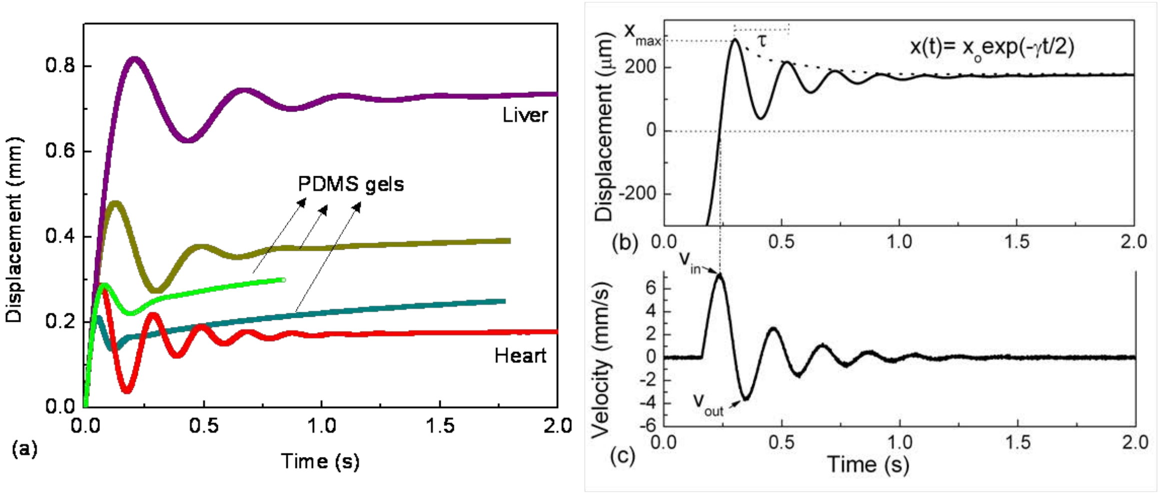

Figure S1. Indenter displacement vs. time response from dynamic impact indentation of soft biological tissues and PDMS gels with 2:1 stoichiometry and 50% solvent loading differing only in solvent MW. From these raw data, one can visually compare the maximum penetration depths (measure of impact resistance) and the number of impact cycles (related to energy dissipation rate). (b) Typical indenter displacement vs. time response, from which maximum penetration depths $x_{\max}$ and quality factor Q are calculated. Q is defined as $Q=2\pi/\tau\gamma$ where τ is the measured period of oscillation and $\gamma/2$ is the inverse of the decay time of the pendulum calculated by modelling the pendulum motion as a damped harmonic oscillatory motion and fitting $x(t) = x_o exp(-\gamma t/2)$ to its local maxima. (c) Indenter velocity vs. time, calculated as the first derivative of displacement with respect to time, producing the impact and rebound velocities, v_{in} and v_{out}, from which energy dissipation capacities K are calculated.

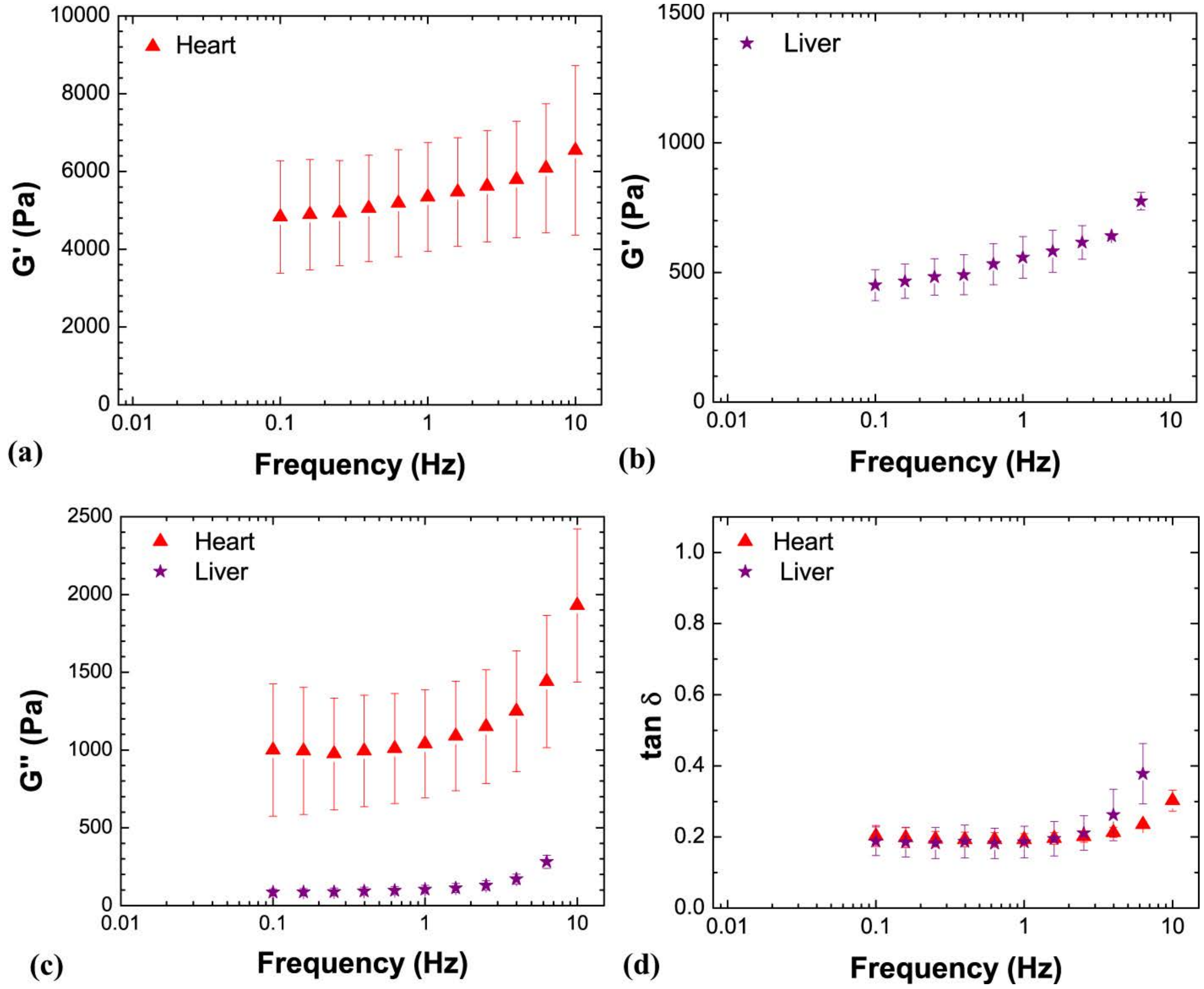

Figure S2. Storage modulus *G'* (a,b) loss modulus *G"* (c) and tan *δ* (d) of heart and liver tissue exhibit frequency dependence.

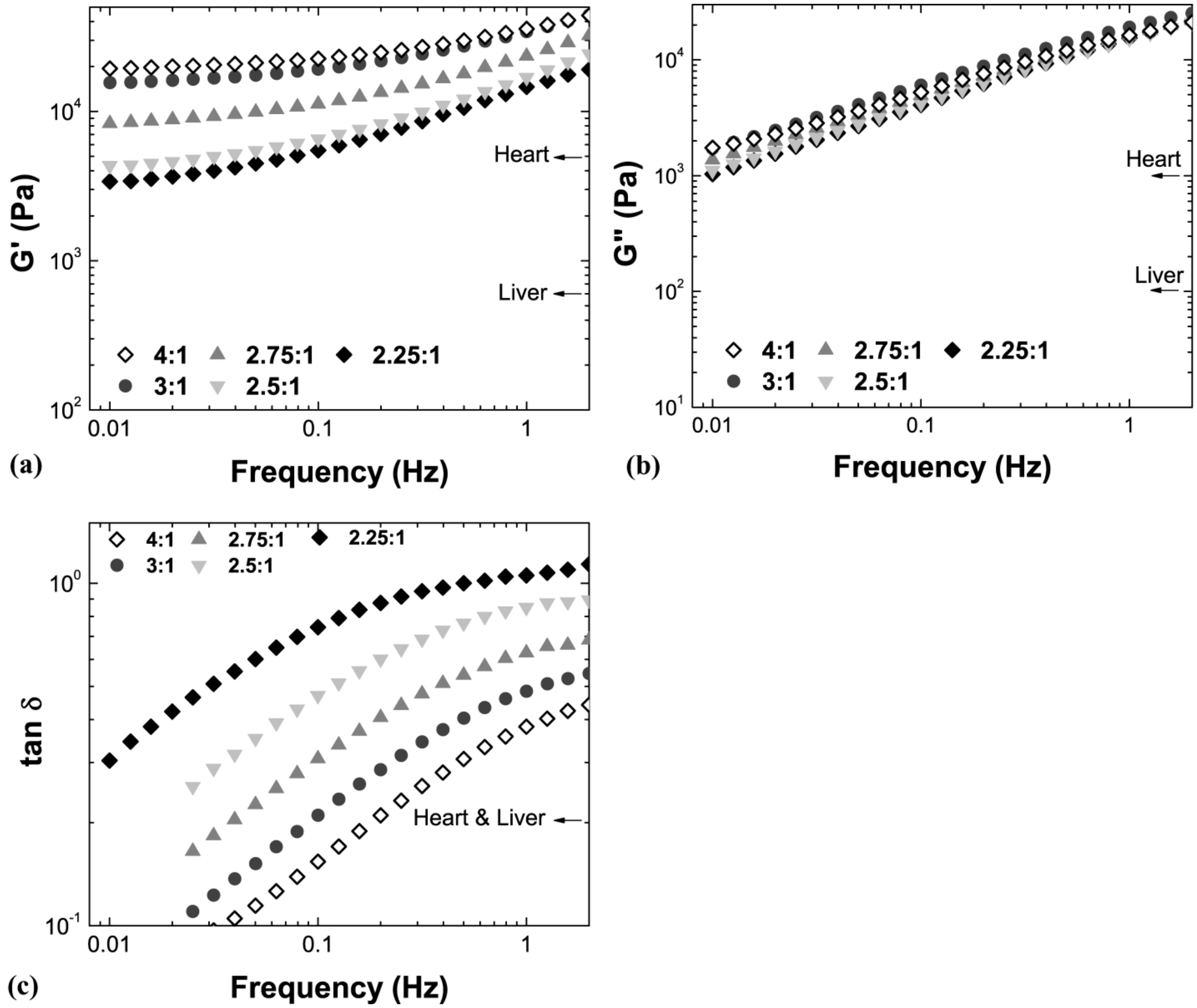

Figure S3. Effect of stoichiometric ratio of silane:vinyl groups on (a) storage modulus *G'* and (b) tan *δ* of PDMS gels containing 60 vol% of 308 kg/mol solvent, compared to heart and liver tissues.

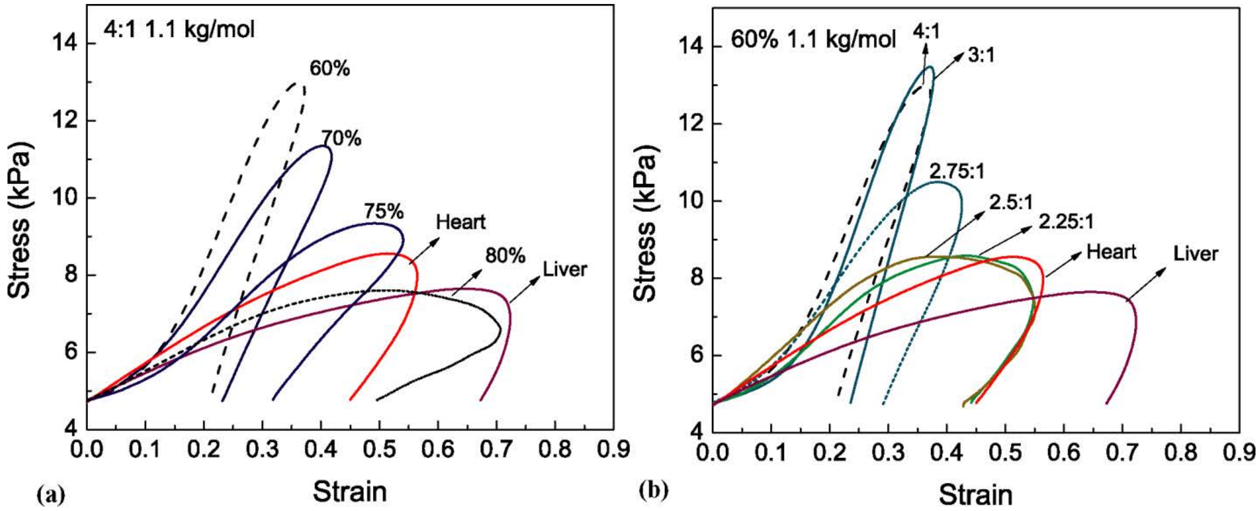

Figure S4. Representative estimated stress vs. strain responses at an impact velocity of 0.7 cm/s (corresponding to F_{acc}= 15 mN) as a function of (a) solvent loading % for PDMS gels with silane:vinyl stoichiometric ratio of 4:1 and solvent molecular weight of 1.1 kg/mol, (b) stoichiometric ratio of silane:vinyl groups for PDMS gels with 60 vol% 1.1 kg/mol molecular weight solvent.